

**RERTR 2011 — 33rd INTERNATIONAL MEETING ON
REDUCED ENRICHMENT FOR RESEARCH AND TEST REACTORS**

**October 23-27, 2011
Marriott Santiago Hotel
Santiago, Chile**

**Interfacial Strength of Al/Al and Al/Zr/DU-10wt%Mo Subject to
Different Loading Modes**

C. Liu, M.L. Lovato, and W.R. Blumenthal
Materials Science and Technology Division
Los Alamos National Laboratory, Los Alamos, NM 87545, USA

ABSTRACT

Compact tension (CT) experiments were conducted with fixtures that allowed mode-I (tensile opening mode), mode-II (shearing mode), and mixed-mode loading to measure the interfacial strength between HIP-clad Al and Al, and Al and Zr/DU-10wt%Mo. Specimens were made with the same HIP process used for making thin composite foils, but instead used 25 mm thick Al-6061 cladding that allowed specimens to be gripped without adhesives. Three configurations of specimens were tested: (1) Al/Al specimens with a pre-crack along the seam; (2) specimens containing both a Zr/DU-10wt%Mo layer and an Al/Al seam along part of the interface; and (3) specimens containing only a Zr/DU-10wt%Mo layer at the interface, but with a pre-notch along part of the interface. Digital image correlation (DIC) was used to measure full-field deformations during the test. The results show that mode-I loaded interfaces exhibit the weakest strength and the widest scatter. The strength increases when more shearing component is introduced.

1. Introduction

A series of compact tension (CT) experiments, combined with the Arcan loading fixture, were conducted to study and measure the interfacial strength between HIP-clad Al and Al, and Al and Zr/DU-10wt%Mo. The Arcan fixture allows different loading modes to be applied to a specimen from mode-I (tensile opening mode) to mode-II (shearing mode). Specimens were obtained by sandwiching a thin foil of Zr/DU-10wt%Mo between two thick (25mm) Al-6061 blocks and applying the same HIP process that is used for making thin (1mm) Al/Zr/DU-10wt%Mo foils. Three types of CT specimens were tested: (1) specimens with a pre-crack along an Al/Al only seam; (2) specimens containing both a Zr/DU-10wt%Mo layer and an Al/Al seam along part of the interface; and (3) specimens containing only a Zr/DU-10wt%Mo layer at the interface, but with a pre-notch along part of the interface. Three loading angles were tested: 0° (mode-I), 45° (mixed-

mode), and 90° (mode-II shear). For the cases of 45° (mixed-mode) and 90° (mode-II), the specimens with Zr/DU-10wt%Mo layer in the middle and a pre-notch along one of the interfaces are also subject to either positive or negative shear. Digital image correlation (DIC) was used to obtain full-field displacements and strains during the test.

2. Experimental Set-up

The interfacial fracture toughness has been shown to strongly depend on the mixity at the crack tip. The crack tip mode mixity is the ratio of the shearing deformation parallel to the interface to the opening deformation perpendicular to the interface.

To investigate the effect of crack tip mode mixity on interfacial failure, we use the compact tension (CT) specimen combined with the Arcan loading fixture, as shown in Fig.1. The CT specimen, shown in Fig.1(a), has a rectangular shape and the Zr/dU-10%Mo layer is located at the center. A pre-crack is machined along one of the interfaces. The Arcan loading fixture has two identical pieces and each piece has a series of holes, where loading pins can be inserted. As shown in Fig.1(a), these holes form a circle and the pair of holes used for loading pins is a diameter of the circle. The initial interfacial crack tip is located at the center of the circle. By varying the pairing of pinholes, different mode mixities at the initial crack tip can be achieved, from pure opening to pure shearing. Meanwhile, by flipping the CT specimen, or equivalently by changing the orientation of the crack (toward right or toward left), both positive and negative shear can be achieved. Figure 1(b) presents the photograph of the actual setup, where the CT specimen is loaded in pure mode-II (shearing mode).

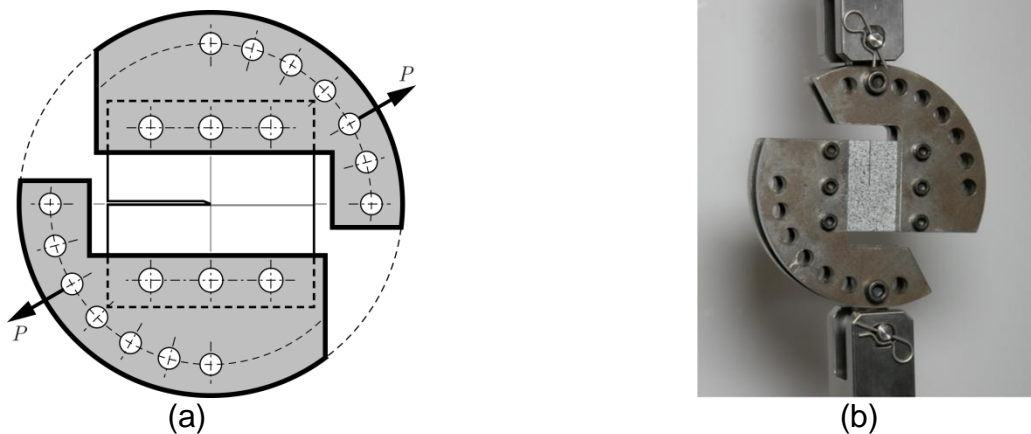


Figure 1: (a) Compact tension (CT) specimen and the Arcan loading fixture; (b) Photograph of the setup.

Three different CT sample configurations are considered and these three sample types are shown in Fig.2: (a) Specimens with a pre-crack along the Al/Al seam (named as Al-Al-notch sample); (b) specimens containing both a Zr/DU-10wt%Mo layer and an Al/Al seam along part of the interface (named as Al-DU-corner sample); and (c) specimens containing only a Zr/DU-10wt%Mo layer at the interface, but with a pre-notch along part of the interface (named as Al-DU-notch sample). The specimens shown in Fig.2(a) are

used for measuring the strength of the bonding of Al and Al from the HIPing process, the samples shown in Fig.2(b) are for studying the strength of material at the tip of the Zr/DU-10wt%Mo layer, and the samples shown in Fig.2(c) are for measuring the strength and toughness of the Al/Zr/DU-10wt%Mo interface, where an interfacial crack is present. Three different loading angles are also considered: 0° (mode-I), 45° (mixed-mode), and 90° (mode-II shear). For the cases of 45° (mixed-mode) and 90° (mode-II), the specimens shown in Fig.2(c) can be subject to either positive or negative shear depending on the location or the orientation of the pre-notch.

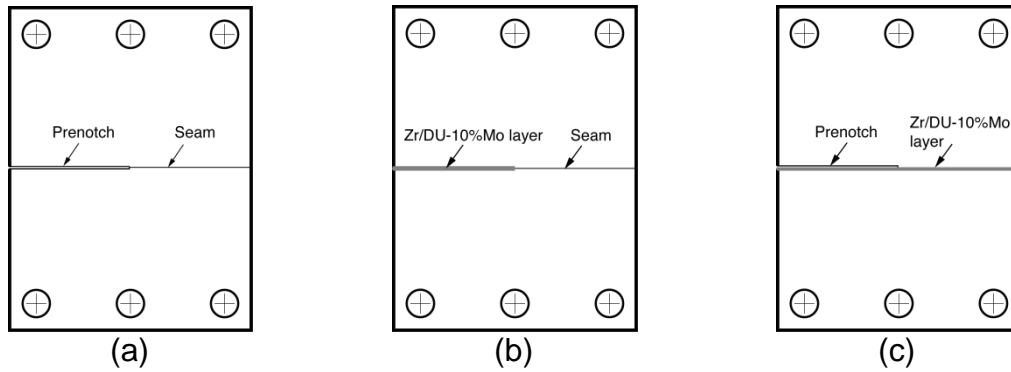


Figure 2: Three types of CT samples tested: (a) Al-Al-notch (b) Al-DU-corner and (c) Al-DU-notch.

In this investigation, we used the digital image correlation (DIC) technique to obtain the deformation field on the specimen surface. This technique relies on the computer vision approach to extract the whole-field displacement data, that is, by comparing the features in a pair of digital images of a specimen surface before and after deformation.

An INSTRON 1125 screw-driven load frame loaded the specimens at a constant crosshead of 0.25mm/minute. The applied tensile load and the crosshead displacement were monitored and recorded at a sampling rate of 10 Hz. A random speckle pattern was printed onto the specimen surface by first depositing a very thin white background and then spraying a black paint. A CCD camera, with the resolution of 1628 x 1236 pixels, was setup in front of the specimen. A series of images was captured during the test at the framing rate of 5 frames/second. All experiments were conducted in ambient temperature (21°C). For every sample configuration and loading angle, two tests were conducted, so there are total of 22 tests in this series of experiments.

3. Results and Discussion

Mode-I loading:

Figure 3 presents the mode-I (opening mode) strength measurements of all three types of specimens shown in Fig. 2. The strength is defined, to be consistent for all configurations and loading angles, as the maximum applied load divided by the overall cross-section area of the specimen, but this definition does not account for the area of notches. Therefore the average interfacial strength for the notched specimens shown in Figs. 2(a) and (c) will be twice the strength values presented in Fig. 3.

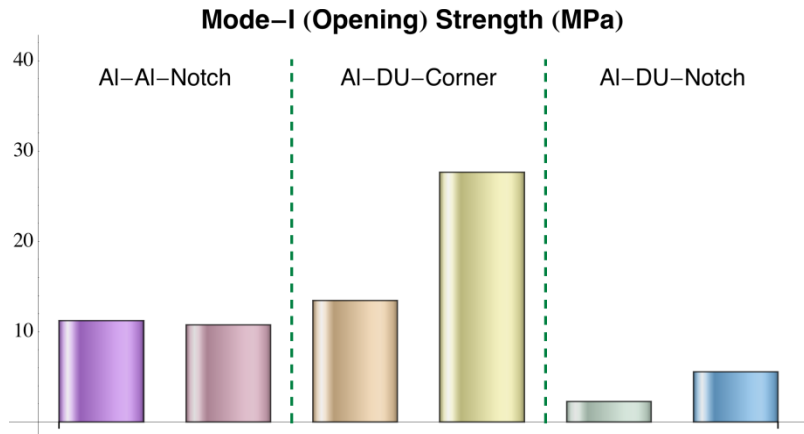


Figure 3: Strength measurement of three different sample types subject to mode-I loading.

The manner in which the specimen failed was also recorded by either camera images captured during the test or by inspection of the failed specimens after the experiment. For the Al-Al-notch specimens, subject to mode-I load, a very small amount of crack growth was observed followed by brittle failure along the Al/Al interface. Figure 4 presents the failure sequence of one of the Al-Al-notch specimens. Figure 4(a) shows the initial state of the specimen; Figure 4(b) is the moment prior to brittle failure where a very small amount of crack growth can be seen; and Figure 4(c) shows the sample after the instant of brittle failure. Because the framing rate of the camera is limited, only a fuzzy image of the sample is captured as the pieces flew apart.

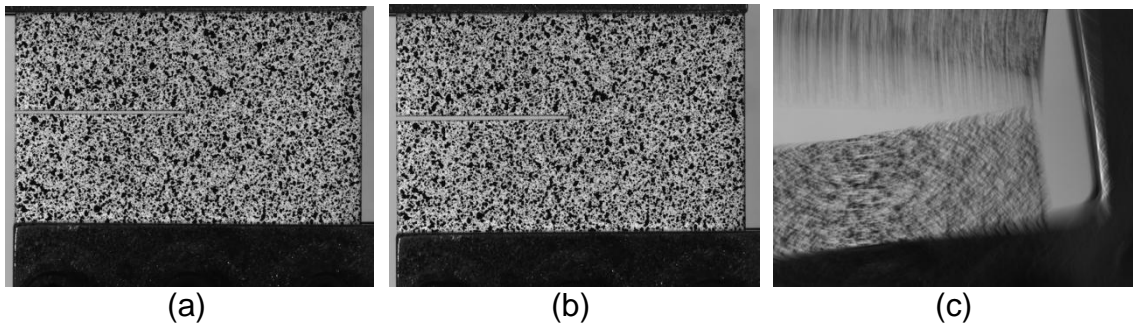


Figure 4: Failure sequence of an Al-Al-notched specimen in mode-I loading: (a) initial image, (b) image of the specimen prior to the moment of failure, and (c) sample image after brittle failure.

The strength of the Al-DU-corner specimens, when subject to mode-I load, exhibit wide scattering, as shown in Figure 3. Note that the strength of one of the Al-DU-corner specimens is very close to that of the Al-Al-notch specimens, which indicates that the strength of this specimen was controlled by the Al/Al bonding alone and that the contribution of the bond between Al and the Zr/DU-10wt%Mo layer is negligible in this case. The other Al-DU-corner specimen exhibits much higher strength compared to any other mode-I specimens shown in Figure 3. Figure 5(a) shows the failure pattern of the weaker Al-DU-corner sample, where one can see the interfacial cracks along both the upper and the lower interface between the Al and the Zr/DU-10wt%Mo layer, as well as a crack along the Al/Al seam in front of the corner of the Zr/DU-10wt%Mo layer. Figure

5(b) shows the failure of the stronger Al-DU-corner sample, which fails in a much more brittle and dynamic manner.

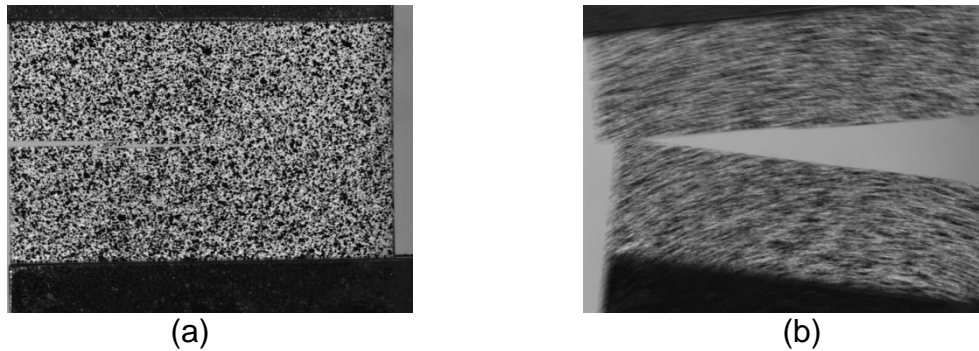


Figure 5: Failure patterns of (a) the weaker Al-DU-corner specimen and (b) the stronger Al-DU-corner sample.

Finally, the strength of the Al-DU-notch specimens subject to mode-I loading is the lowest of all other specimens tested and the scatter is also large. The failure patterns for the weaker and the stronger samples are again different, as shown in Figure 6. Whether failure initiates from the notch tip or from the back of the specimen cannot be determined with the imaging system because the brittle failure proceeds too rapidly.

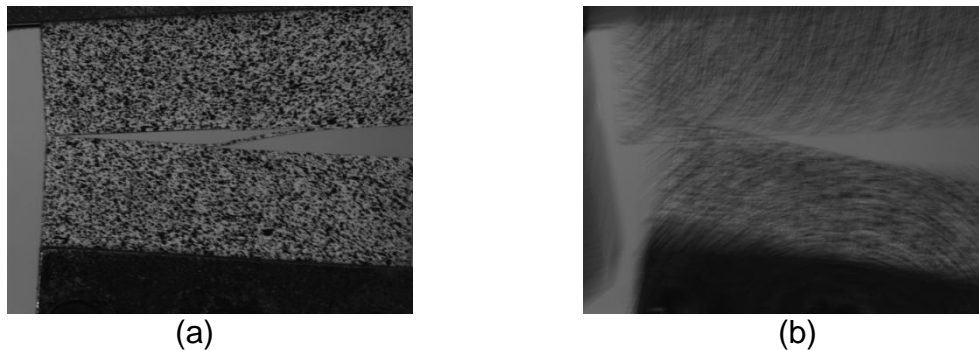


Figure 6: Failure patterns of (a) the weaker Al-DU-notch specimen and (b) the stronger Al-DU-notch sample.

Mixed-mode loading:

The strength of samples subject to mixed-mode loading, where the loading axis is at 45° to the interface of the CT specimen, are shown in Figure 7. Every type of specimen subject to mixed-mode loading is stronger than when it is subject to mode-I loading, except for the one Al-DU-corner sample shown in Figure 3.

Al-Al-notch specimens clearly show an amount of crack growth before they fail. The Al-DU-corner specimens fail in a brittle, dynamic fashion without visible crack growth. When shearing deformation was applied to the Al-DU-notch specimen, it was applied in both “positive” and “negative” shearing directions. By positive shearing, we mean that in this bi-material system, where the Al is sitting on top of the Zr/DU-10wt%Mo layer and

an interfacial crack is situated along the interface, the shearing direction above the Al/Zr/DU-10wt%Mo interface in front of the notch tip is pointing away from the notch tip. If the shearing direction is pointing toward the notch tip, we call the situation negative shearing. As shown in Figure 7, the strength of the Al-DU-notch samples in both positive and negative shearing is essentially the same and they all exhibit brittle failure.

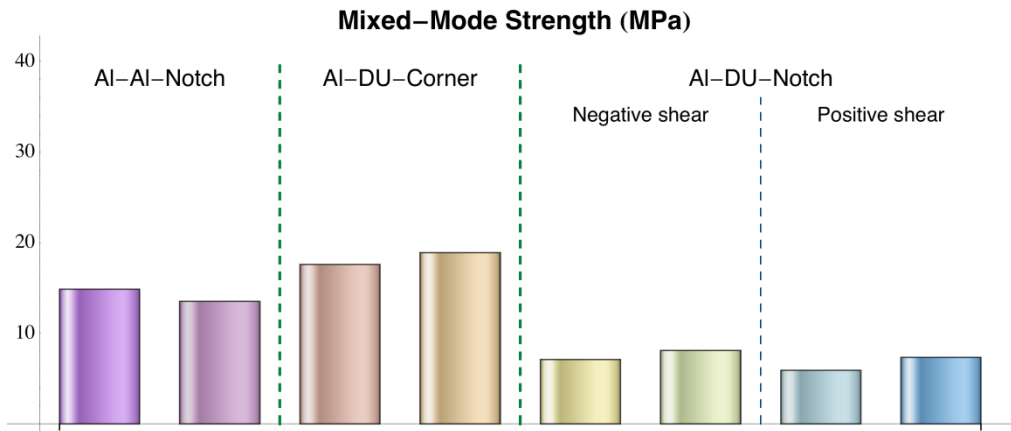


Figure 7: Strength measurement of three different sample types subject to mixed-mode loading.

Mode-II loading:

In mode-II loading, the external load is applied in the direction parallel to the Al/Al seam or the Al/Zr/DU-10wt%Mo interface, so that the notch-tip in the Al-AI-notch specimens and the Al-DU-notch specimens and the corner-tip in the Al-DU-corner specimens are initially subject to shear stress. The measured strength of all the samples is shown in Figure 8. The overall trend is that for all types of specimens subject to mode-II load, the strength is higher than that of both the mode-I load and the mixed-mode load as shown in Figures 3 and 7.

When specimens were subject to mode II shear-dominated loading, both the maximum strength at which the sample fails and the appearance of failure of these samples are different than when some portion of the loading is tensile. For the Al-AI-notch specimens in mode II loading (shearing mode), an amount of crack growth was observed during loading, but then the specimens did not fail. Instead, the bolt-holes gripping the specimen tore, so that the strength measurements shown in Figure 8 for the Al-AI-notch specimens only represent the value at which the pre-notch starts to propagate and the true strength value is some amount higher than this value. Similarly for the Al-DU-corner samples in mode II loading, neither the Al/Al seam nor the Al/Zr/DU-10wt%Mo interface failed, but instead the bolt holes fail. Therefore, we use the “>” symbol to indicate that the strength of the Al-DU-corner samples is no less than the values shown in Figure 8.

When the Al-DU-notch samples were subject to mode-II shearing in the negative sense, the situation is similar to that of the Al-AI-notch specimens, where a small amount of crack growth occurred along the Al/Zr/DU-10wt%Mo interface and the specimen never failed. The difference between Al-DU-notch samples and the Al-AI-notch samples when

subject to negative shear is that we observe extensive deformation in front of the notch in the Al-DU-notch samples. On the other hand, when the Al-DU-notch samples were subject to the positive shearing load, extensive deformation in front of the notch was also observed, but this extensive deformation was followed by brittle failure. Thus the strength measurement shown in Figure 8 for Al-DU-notch sample subject to positive shear represents the true strength value.

The distinction of the failure behavior of Al-DU-notch sample subject to either negative or positive shear highlights the effect of the direction of shear at the tip of the notch when large deformation is involved. For infinitesimal deformation, the direction of the shear stress at the notch tip has no effect on the material failure. However, for finite or large deformation, even when the globally applied load is predominantly shear, the local deformation near the notch tip will involve some normal component. This normal component is compressive for negative shear, and it is tensile for positive shear.

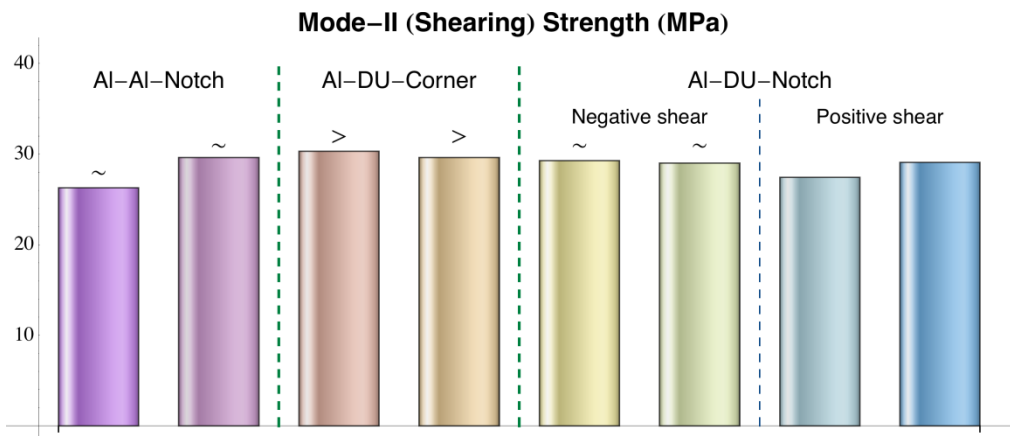


Figure 8: Strength measurement of three different sample types subject to mode-II loading.

Deformation field and related results

In the preceding sections, the global strength measurement was presented and the observation of the appearance of the failure process was discussed. The strength measurement can be obtained from the global loading monitored by the load cell. The deformation or the displacement measurement is a challenging issue. Although we monitored and recorded the crosshead motion of the test machine, such a measurement does not represent the deformation or displacement experienced by the test specimen, since the compliance of the test machine and loading fixture also contributes to the motion of the crosshead. In this series of experiments, the displacement experienced by the CT specimen was determined using the optical digital image correlation (DIC) technique. Some of these results will be presented here.

DIC relies on the computer vision approach to extract the whole-field displacement data by comparing the features in a pair of digital images of a specimen surface before and after deformation. The features used in this series of experiments are the random speckle pattern on the sample surface. The random speckle pattern was made by first

painting a thin layer of white background and then by spraying a black paint onto the surface. Figure 9 shows the displacement fields, obtained by using DIC, of the Al-Al-notch specimen subject to mixed-mode load very close to the moment of failure. The contour plot on the left is the displacement component in the horizontal direction and the contour plot on the right the displacement component in the vertical direction.

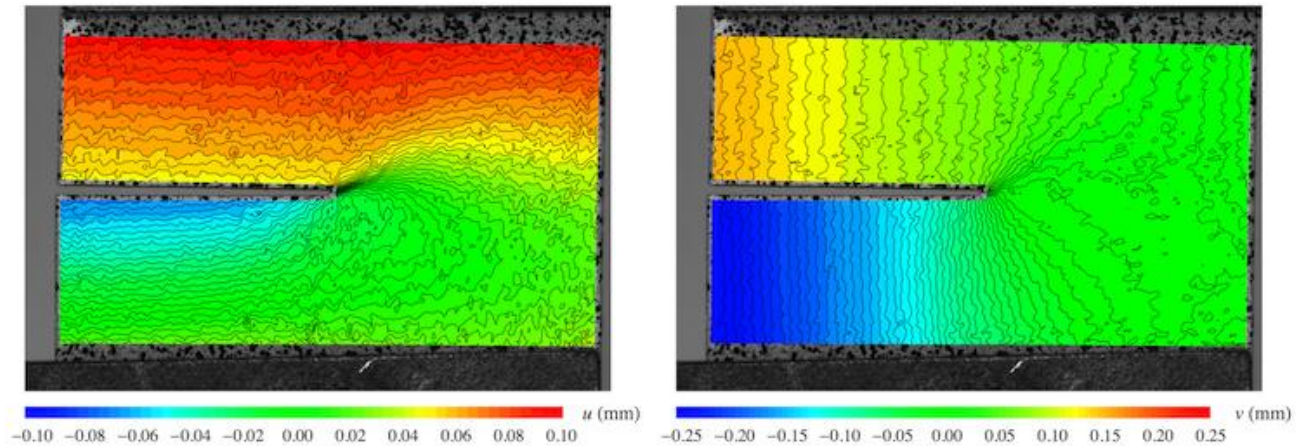


Figure 9: Displacement fields on the surface of Al-Al-notch specimen obtained from DIC.

One use of the DIC data shown in Figure 9 is to provide displacement information over a region on the surface of the specimen. One such region is illustrated in Figure 10(a) as the yellow dashed line. Among all the points from the DIC data, we can identify the displacements along the boundary lines on the top and the bottom of the region indicated as pink lines. The average relative motion of these two lines can be used as a measure of the displacement experienced by the CT specimen during the testing. As a result, we can plot the applied load, normalized by the cross-section area of the specimen, as a function of the relative displacement as shown in Figure 10(b). The area underneath the curve represents the energy absorbed by the CT specimen and can be used as one characteristic of the interface.

The shape of the curve shown in Figure 10(b) also provides information regarding the characteristics of the CT specimen and the interface. Figure 11 presents the variation of the normalized applied load as function of the displacement determined according to the scheme just mentioned for two types of the CT specimens. One is the Al-Al-notch specimen subject to mixed-mode load and the other is the Al-DU-notch specimen subject also to the mixed-mode load with the positive shear component. The distinctive response of these two types of samples is apparent. The Al-DU-notch specimen, when subject to mixed-mode load, behaves in an elastic/brittle fashion, where the curves are linear up to the point of final failure.

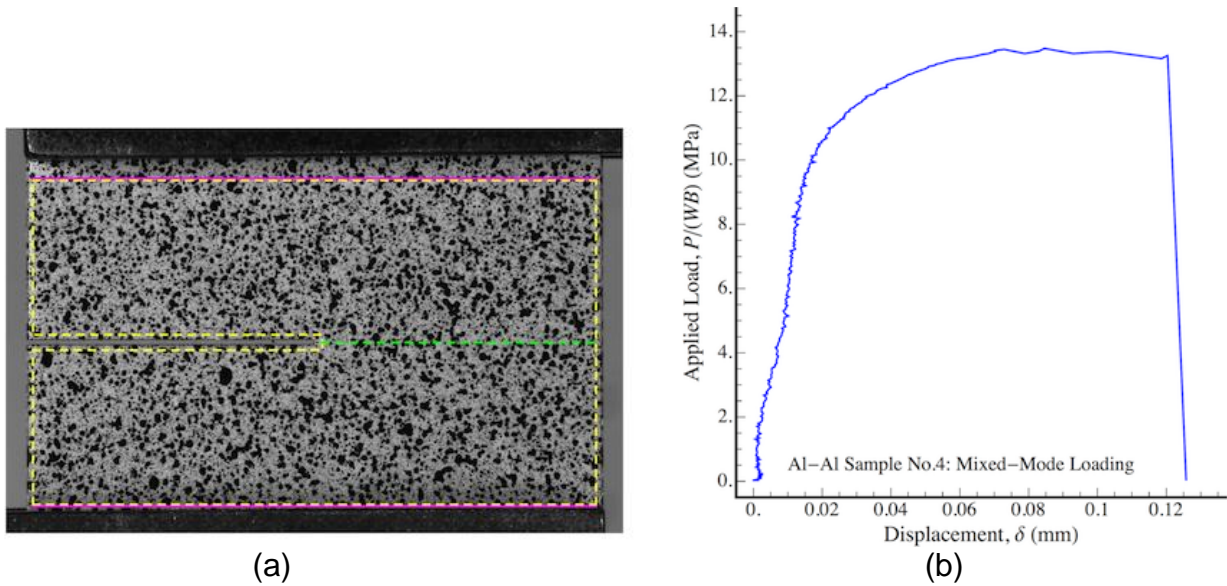


Figure 10: (a) Extraction of the displacement experienced by the CT specimen from DIC data.
 (b) Variation of applied load as function of displacement of the CT specimen.

On the other hand, the Al-Al-notch specimen under mixed-mode loading resembles the behavior of elastic/plastic material, where following the apparent linearly elastic deformation, there is a very large portion of nonlinear deformation prior to the final failure. The contributing factor for such nonlinear deformation includes the plastic deformation near the tip of the notch and the small amount of crack growth along the Al/Al interface.

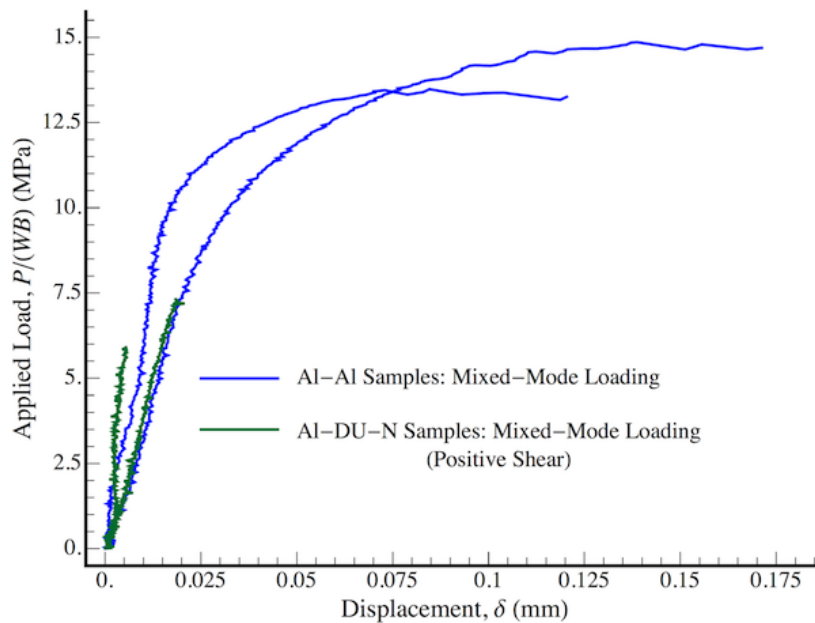


Figure 11: Variation of normalized applied load as function of displacement experienced by the Al-Al-notch specimen and the Al-DU-notch specimen subject to mixed-mode-loading.

The strain fields on the specimen surface can also be obtained based on the displacement fields obtained from DIC. Figure 12 shows the contour plots of the strain fields of the Al-Al-notch specimen subject to mixed-mode load close to the moment of failure. From the left to the right, these contour plots represent the normal strain in the horizontal direction, the normal strain in the vertical direction, and the shear strain. The quantitative measurement of the local deformation fields will provide useful information to FEA simulations to validate the numerical models.

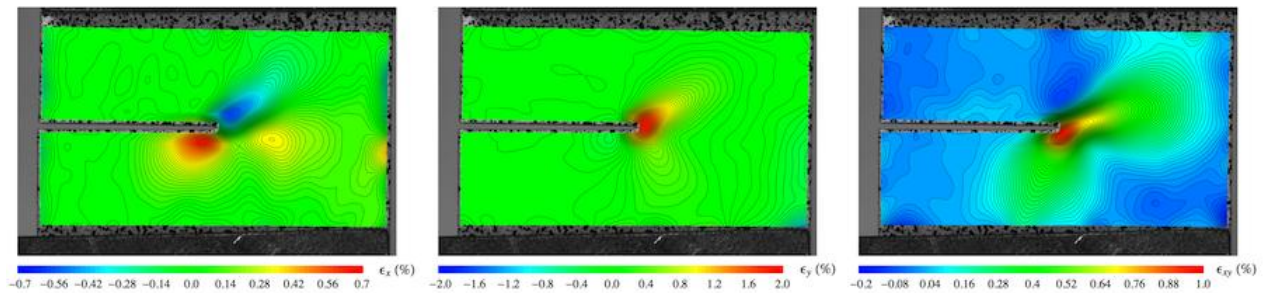


Figure 12: Contour plots of the strain fields on the surface of Al-Al-notch specimen subject to mixed-mode loading.

4. Summary

A total of 22 compact tension (CT) tests were conducted. We investigated three different sample configurations, the Al-Al-notch, the Al-DU-corner, and the Al-DU-notch specimens. Three different loading angles were also evaluated: the mode-I (tensile opening) load, the mixed-mode load, and the mode-II (shearing) load. The DIC technique was applied to obtain full-field deformation contour maps of the specimen surface during the test.

We observed that except one outlier in Al-DU-corner specimen, the strength of all the specimens increased when more shearing component was introduced in the loading. Subject to the mode-I (opening) load, the specimens (or the interfaces) exhibit the weakest strength and the widest scattering. This observation suggests that we may focus on the mode-I (opening) loading mode for future investigations of the bonding strength of various interfaces.

DIC is a data-rich technique and we are still in the process of processing the DIC data of all the tests and the details of those results will follow in future publications.

5. Acknowledgements

The authors would like to acknowledge the financial support of the US Department of Energy Global Threat Reduction Initiative Reactor Convert program. Los Alamos National Laboratory, an affirmative action equal opportunity employer, is operated by Los Alamos National Security, LLC, for the National Nuclear Security Administration of the U.S. Department of Energy under contract DE-AC52-06NA25396.